Hindawi Publishing Corporation
Journal of Nanomaterials
Volume 2010, Article ID 620505, 6 pages
doi:10.1155/2010/620505

Research Article

Formation of Au/Pd Alloy Nanoparticles on TMV

Jung-Sun Lim,[1] Seung-Min Kim,[2] Sang-Yup Lee,[3] Eric A. Stach,[2] James N. Culver,[4] and Michael T. Harris[1]

[1] *School of Chemical Engineering, Purdue University, West Lafayette, IN 47906, USA*
[2] *School of Materials Engineering, Purdue University, West Lafayette, IN 47906, USA*
[3] *Department of Chemical, and Biomolecular Engineering, Yonsei University, Seoul 120-749, South Korea*
[4] *Center for Biosystems Research, University of Maryland Biotechnology Institute, College Park, MD 20742, USA*

Correspondence should be addressed to Michael T. Harris, mtharris@ecn.purdue.edu

Received 22 July 2009; Revised 18 November 2009; Accepted 8 January 2010

Academic Editor: Michael Wong

A gold-palladium (AuPd) solid solution alloy was successfully deposited on the genetically engineered tobacco mosaic virus (TMV1Cys) by the biosorption of Au(III) and Pd(II) precursors and the reduction of the Au(III) and Pd(II) to their respective metals or metal alloy. The resulting morphologies of alloy nanoparticles deposited on the TMV1Cys were observed with transmission electron microscopy (TEM), and the AuPd alloy formation was supported with surface plasmon resonance (SPR) and selected area electron diffraction (SAED). In addition, selected alloy nanoparticles on the TMV1Cys were analyzed further with electron energy loss spectroscopy (EELS) to confirm the presence of gold and palladium. Our result implies that biotemplated metal mineralization is a potentially useful methodology to prepare alloy nanoparticles.

1. Introduction

Electric and optical properties of the metal/semiconductor nanoclusters are tunable depending on their size and shape [1–3]. To take full advantage of the quantum size effect, various approaches have been investigated to synthesize the nanoscaled objects with tunable properties. Using biologically driven macromolecules and their self-assembled structures as templates is one very promising methodology to prepare nanoscale organic-inorganic hybrid structures, such as nanowires [4–19] or patterned arrays [10, 20]. Unlike CVD or water in oil emulsion synthesis routes that require extreme processing conditions (such as a vacuum, high temperature, and harsh chemical process), biotemplated nanomaterial synthesis is able to control the nanoscale structures in relatively mild processing conditions. The self-assembly of the proteins provides well-defined tubular biotemplates for nanowire synthesis, such as the tobacco mosaic virus and M13 bacteriophage. Genetic engineering enables the manipulation of the self-assembled template structure and its surface functionalities, providing the opportunity for selective deposition of materials on the surface of the biotemplate.

The tubular biotemplates have demonstrated surface mineralization of metal/semiconductors leading to the formation of nanowires or patterned nanoarrays. For example, the mutants of M13 showed selective semiconductor crystallization [6, 7, 9] and were exploited for the preparation of flexible film electrodes by coating metal deposited on their assembly [10]. Additionally, various metal depositions were achieved on TMV and related mutants to form discrete and continuous metal coatings [11–14]. The self-organization of TMVs on a gold substrate followed by nickel plating on the virion surface produced nanopatterned electrodes with high surface area [20]. Potential applications of the palladium nanocluster-deposited TMV were demonstrated in hydrogen gas-sensing [21], and memory storage [22]. The above examples suggest that biotemplated mineralization is promising for the preparation of nanostructured electric devices.

Various Class B metal alloys have been used as high temperature resistors, hydrogen permeation membranes, multilayer capacitors, and magnetic memory storage materials [23]. One of the most important factors for the application of alloy metals is controlling the composition of the alloy in wide ranges. As the size of the structure approaches

the nanometer scale, a more reliable method to control the alloy composition is required. Biomolecule-mediated metal cluster nucleation is advantageous for the alloy composite synthesis because the heterogeneous nucleation of metal ion can be controlled by the biomolecule and the homogeneous mixing of various ionic metal salts are possible in the aqueous medium where the biomolecules are suspended. TMV has structural benefits to investigate the biomediated alloy mineralization. TMV is a self-assembly of ~2130 identical coat proteins and a single strand of RNA to form a tubular structure. Thus, the external surface of TMV1Cys has repeating unit surface of identical $2.3 \times 3.5\ \text{nm}^2$ with affinity to the metal ions after genetic modification [13, 14, 24, 25]. Onto this surface, successful biosorption of Au(III) and Pd(II), respectively, has been demonstrated [26].

Several researchers have investigated the mechanism of metal deposition on TMV. Dujardin et al. [11] hypothesized that the anionic metal ion complexes will be attracted to the positively charged surface functionalities of TMV followed by the selective reduction of the ionic form of the metal clusters on the virion surface. Lee et al. [13, 14] reported the enhanced metal mineralization on the genetically engineered mutant TMV with couple of extra cysteines (TMV2Cys) whose sulfhydryl groups on the surface attracted the metal ions. Lim et al. [26] investigated the Pd(II) and Au(III) biosorption on the TMV1Cys. The enhanced palladium ion loading improved the palladium deposition from discrete cluster-type deposition to fully-layered coatings.

As an extension of the previous work [26], current research investigates the simultaneous biosorption of Pd(II) and Au(III) ions, leading to the gold-palladium alloy deposition on the genetically modified tobacco mosaic virus (TMV1Cys). The Au(III) and Pd(II) biosorption on the TMV1Cys were utilized to uptake the different molar ratios of Au(III) and Pd(II) from the medium. The biosorbed Au(III) and Pd(II) ions on the TMV1Cys were subsequently reduced by the reducing agent to mineralize the alloy nanoclusters on the virion. The resulting morphologies of the gold-palladium alloy particles deposited on TMV were imaged with transmission electron microscopy (TEM). Additionally, the metal coated TMV1Cys were analyzed with a surface plasmon resonance (SPR) at 525 nm [3] and the selected area electron diffraction (SAED) of the metal clusters to support the formation of alloy on the virion. The sample was analyzed with electron energy loss spectroscopy (EELS) to demonstrate the existence of Pd and Au atoms in nanoclusters.

2. Experiment

2.1. Au(III) and Pd(II) Ion Uptake. Hydrogen tetrachloroaurate(III) (Aldrich,99.9 + %) and sodium tetrachloropalladate(II) (Aldrich, 98%) were used as sources of the metal ions. As a biotemplate, 11.4 mg/ml of TMV1Cys stock was harvested from the infected tobacco leaves [27, 28]. UV-Vis spectroscopy (Cary 100 Bio, Varian) was used to measure the change of metal ion concentration before and after biosorption. The Au(III) ion has a characteristic UV-Vis absorption at 313 nm [29], and the absorption intensity was

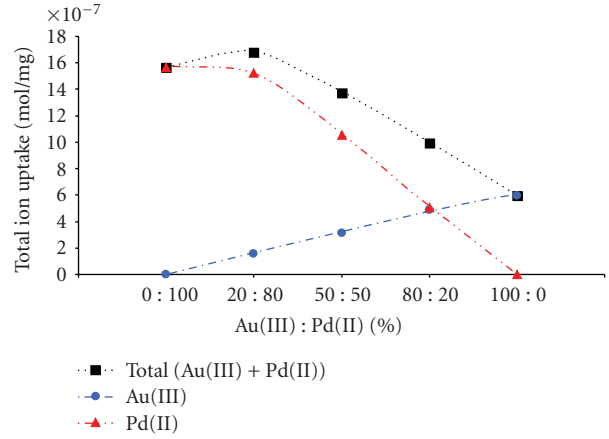

Figure 1: The Au(III) and Pd(II) uptake on the TMV1Cys.

linearly increased with the concentration. For the Pd(II) ion, UV-Vis absorption at 252 nm [30] was used to measure the concentration. In addition, a 0.015 M sodium chloride solution was used as a base medium for the biosorption of metal ions in order to suppress substitution of the chloride ions in the metal ion complex with the hydroxide ions over time.

The sorption of Au(III) and Pd(II) ions on TMV1Cys was investigated. The TMV1Cys concentration was set at 3.8×10^{-2} mg/ml. While the total concentration of Au(III) and Pd(II) mixture was fixed at 2.8×10^{-7} mol/ml, the atomic percentage of Au(III) : Pd(II) was adjusted to be 100 : 0, 20 : 80, 50 : 50, 80 : 20, and 0 : 100. The aqueous mixtures of TMV1Cys and metal salts were aged one hour in dark to reach the sorption equilibrium. For the concentration calibration, all samples were prepared with standard solutions having identical concentrations of Au(III) and Pd(II) in the medium. After aging, samples were centrifuged at 16,000 rpm for 15 minutes (Centrifuge 5417 c, Eppendorf) to separate the supernatant from the virion templates for the determination of free metal ion concentration. Supernatants of samples were scanned with a UV-V is spectrometer to measure the absorption at 252 nm and 313 nm. The differences in the absorbance intensities between a standard sample (without TMV) and TMV-added samples were used to measure the Au(III) and Pd(II) loading on the TMV virion.

2.2. Gold-Palladium Deposition on the TMV1Cys. After aging the mixture of metal ions and TMV1Cys for one hour, the alloy metal deposition was achieved by addition of freshly prepared 2.97×10^{-7} mol/ml dimethylamine borane (DMAB, Aldrich 97%). The gold-palladium alloy nanoparticles deposited on TMV were imaged with transmission electron microscopy (CM10, Philips/FEI). To confirm the alloy formation of gold and palladium on the virion template, the surface plasmon resonance of alloy metal clusters was measured at the wavelength of 525 nm. Additionally, SAED patterns of metal-deposited TMV1Cys were obtained to confirm the presence of a single solid-solution alloy phase

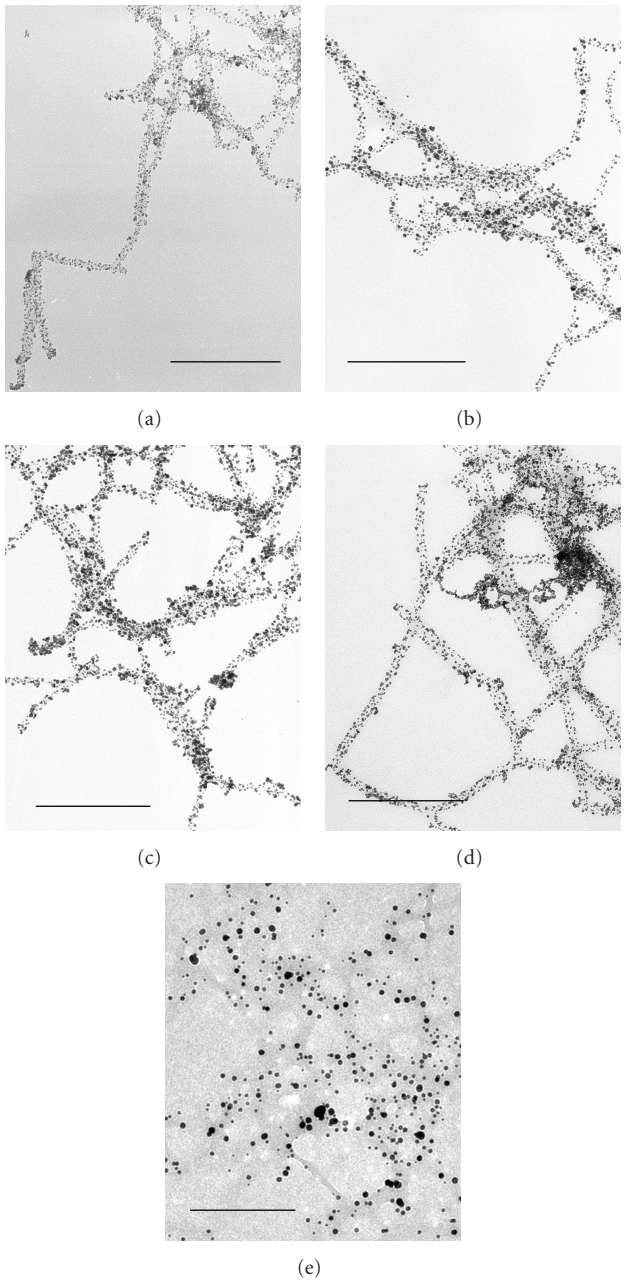

Figure 2: TEM images of AuPd alloy deposited TMV1Cys templates prepared from different Au(III) : Pd(II) percentage of (a) 0 : 100, (b) 20 : 80, (c) 50 : 50, (d) 80 : 20, and (e) 100 : 0 (scale bar: 200 nm).

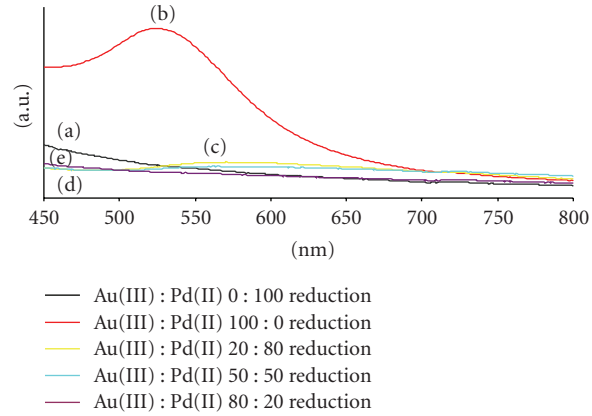

Figure 3: The surface plasmon absorption spectra (at 525 nm) of AuPd alloy deposited TMV1Cys templates prepared from different Au(III) : Pd(II) percentages of (a) 0 : 100, (b) 100 : 0, (c) 20 : 80, (d) 50 : 50, and (e) 80 : 20 (scale bar: 200 nm).

of the face centered cubic (FCC) structure, not the presence of separate gold and palladium phases. A selected sample was analyzed with EELS to confirm the presence of Pd and Au atoms in the nanoclusters.

3. Results

The Au(III) and Pd(II) uptake on the TMV1Cys, under the fixed total metal ion concentration of 2.8×10^{-7} mol/ml, were summarized in Figure 1. When two metal ions, Au(III) and Pd(II), were simultaneously biosorbed on the TMV1Cys, the total amount and the fraction of the Pd(II) : Au(III) were varied. These results strongly suggest that the biosorption of multiple metal ions on the TMV1Cys is potentially tunable.

TMV1Cys was initially suspended in Au(III) : Pd(II) ion mixture solutions (100 : 0, 80 : 20, 50 : 50, 20 : 80, and 0 : 100) and the biosorbed metal ions were subsequently reduced to form AuPd alloy by the addition of DMAB. The resulting morphologies of AuPd alloy decorated TMV1Cys were observed using TEM (Figure 2). The mixture of Au(III) : Pd(II) improved total metal ion loading on the TMV1Cys in comparison to the case where the sole Au(III) precursor was used. Consequently, improved metal coverage was achieved on the virion (Figures 2(b)–2(d)) when compared to the Au(III) only solution (Figure 2(e)), which is in good agreement with the previous work by Lim et al. [26]. There have been reports that the biosorbed Au(III) and Pd(II) showed poor desorption with the charge inversion of sorbent functionalities by pH adjustment. Significant desorption was achieved only when chemicals (thiourea) that form strong ligands with the metals were used in the medium [31, 32]. The cysteine mutant TMVs demonstrated improved surface mineralization in comparison to the wild-type TMV (nonsulfhydryl groups on the external) [13, 14, 26], suggesting the possibility of the complexation of metal precursor/metal with the sulfhydryl groups. The strong affinity of the metals to the sulfhydryl group improves the biosorption properties, which should result in denser alloy cluster mineralization on the TMV1Cys template.

To support the conjecture that the alloys formed as solid-solution nanoparticles, the alloys on the TMV1Cys were analyzed further using the SPR and SAED. The UV-Vis absorptions at 525 nm for the gold, palladium, and gold-palladium alloys are summarized in Figure 3. When Au(III) precursor was used without Pd(II), the gold cluster deposition on the TMV1Cys was recognized by the characteristic SPR absorption peak at 525 nm (Figure 3(b)). In contrast, the depositions of palladium or gold-palladium alloys on the virion (Figures 3(a), 3(c)–3(e)) did not show

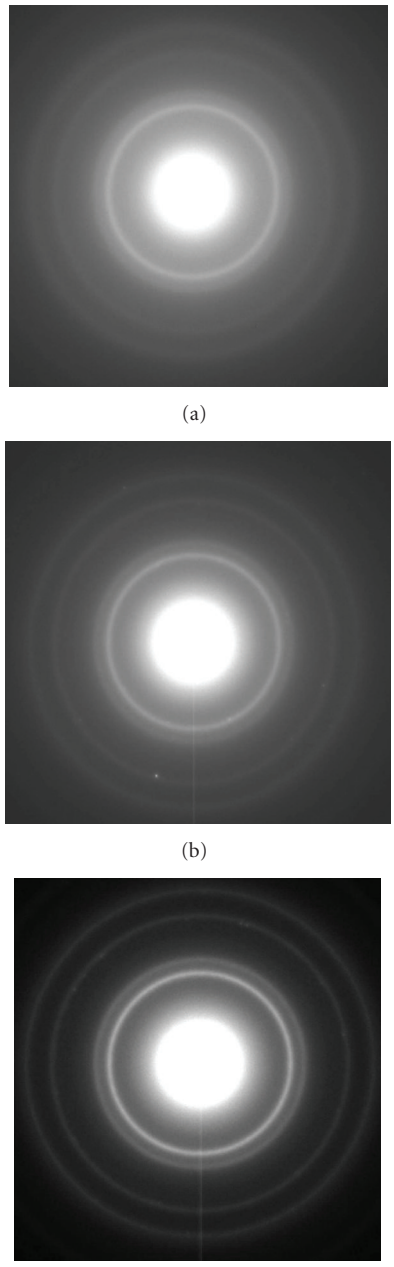

Figure 4: SAED patterns of AuPd alloys prepared from different Au(III) : Pd(II) percentage of (a) 80 : 20, (b) 50 : 50, and (c) 20 : 80.

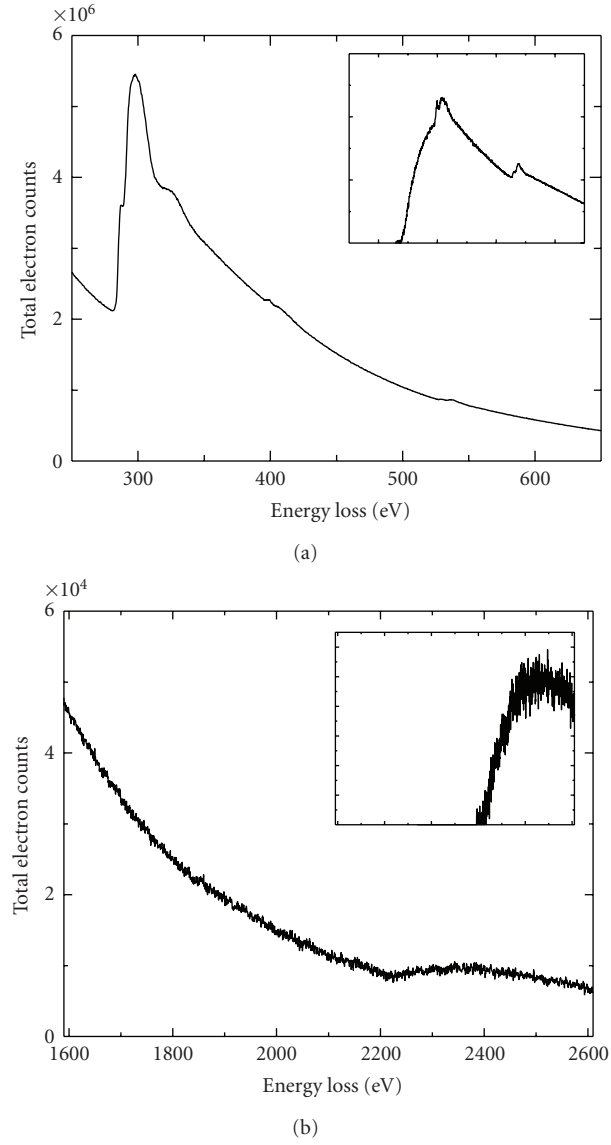

Figure 5: Electron energy loss spectra collected from AuPd (20 : 80) alloy nanoparticles on TMV1Cys, showing existence of (a) Pd at $M_{4,5}$ edge (335 eV) and (b) Au at M_5 edge (2206 eV). Insets are background subtracted electron energy loss spectra at 335 eV and 2206 eV, respectively.

significant absorption peaks at 525 nm. In prior work, Kim et al. [33] demonstrated a significant decrease of gold SPR at 525 nm by AuPd alloying. Similarly, Figure 3 strongly indicates that the AuPd nanoparticles on the TMV1Cys should be predominately an AuPd alloy rather than the phase-separate Au and Pd nanoparticles. The AuPd alloy formation on the TMV1Cys was further supported with SAED. X-ray diffraction (XRD) data reported by Kim et al. [33] showed that the AuPd alloys produced a single phase diffraction signal at 38.7° of (111) plane whereas the separate Pd and Au mixture produced the two diffraction signals of Pd (111) at 39.8° and Au (111) at 38.2°, indicating two different phases. Since SAED of many particles is exactly analogous to XRD and if the gold and palladium are separately mineralized, the FCC (111), (200), (220), and (311) of two metals should produce 8 rings due to the differences between the Au and Pd lattice spacings [34]. However, the diffraction patterns of AuPd alloys on the TMV1Cys (Figure 4) showed only the first four rings, suggesting the AuPd on the sample is a single phase or completely alloyed. In principle, accurate lattice spacing measurement of AuPd alloys with different composition would allow us to at least roughly determine a composition of nanoparticles formed, but in our case uncontrollable experimental errors such as

small variation in objective lens focus and also broadening of diffraction rings from nanosized particles prevented us from doing deeper analysis with diffraction patterns in Figure 3. Instead, in order to further confirm the existence of gold and palladium atoms in the nanoclusters, EELS was performed on AuPd alloy (20 : 80) on TMV1Cys. Electron energy loss spectra were collected from a couple of particles at several spots. Figure 5 shows representative electron energy loss spectra at 335 eV of the Pd $M_{4,5}$edge (Figure 5(a)) and at 2206 eV of the Au M_5 edge (Figure 5(b)), confirming the existence of both Pd and Au [35]. Based on the consistent characterization results by three different approaches, it can be safely concluded that the AuPd nanoparticles on TMV1Cys form a solid solution alloy.

4. Conclusion

As a model study, the biosorption of multiple metal ions on the TMV1Cys was utilized to prepare the biotemplated alloy metal nanoparticles. The Au(III) and Pd(II) ions were simultaneously biosorbed on the TMV1Cys whose uptake ratio could be controlled by varying the initial concentration of Au(III) and Pd(II) in the medium. The deposition of AuPd alloy on the TMV1Cys was achieved by the addition of the reducing agent to samples with different ratios of Au(III) : Pd(II) ion concentration. The formation of AuPd nanocrystal alloys on the TMV1Cys was analyzed using spectroscopic techniques as well as electron diffraction that can clearly indicate the crystalline structure. These results suggest that gold nanoclusters did not segregate, but the gold atoms were mixed with the palladium atoms to form metal alloy nanoclusters. The biosorption of multiple metal ions on the TMV is a potentially useful tool to prepare metal alloy nanoparticles with a tunable alloy ratio.

References

[1] Y.-W. Jun, J.-S. Choi, and J. Cheon, "Shape control of semiconductor and metal oxide nanocrystals through nonhydrolytic colloidal routes," *Angewandte Chemie International Edition*, vol. 45, no. 21, pp. 3414–3439, 2006.

[2] J. Park, J. Joo, G. K. Soon, Y. Jang, and T. Hyeon, "Synthesis of monodisperse spherical nanocrystals," *Angewandte Chemie International Edition*, vol. 46, no. 25, pp. 4630–4660, 2007.

[3] P. Mulvaney, "Not all that's gold does glitter," *MRS Bulletin*, vol. 26, no. 12, pp. 1009–1014, 2001.

[4] J. Richter, M. Mertig, W. Pompe, I. Mönch, and H. K. Schackert, "Construction of highly conductive nanowires on a DNA template," *Applied Physics Letters*, vol. 78, no. 4, pp. 536–538, 2001.

[5] E. Braun, Y. Eichen, U. Sivan, and G. Ben-Yoseph, "DNA-templated assembly and electrode attachment of a conducting silver wire," *Nature*, vol. 391, no. 6669, pp. 775–778, 1998.

[6] S.-W. Lee, C. Mao, C. E. Flynn, and A. M. Belcher, "Ordering of quantum dots, using genetically engineered viruses," *Science*, vol. 296, no. 5569, pp. 892–895, 2002.

[7] C. Mao, C. E. Flynn, A. Hayhurst, et al., "Viral assembly of oriented quantum dot nanowires," *Proceedings of the National Academy of Sciences of the United States of America*, vol. 100, no. 12, pp. 6946–6951, 2003.

[8] C. Mao, D. J. Solis, B. D. Reiss, et al., "Virus-based toolkit for the directed synthesis of magnetic and semiconducting nanowires," *Science*, vol. 303, no. 5655, pp. 213–217, 2004.

[9] S. R. Whaley, D. S. English, E. L. Hu, P. F. Barbara, and A. M. Belcher, "Selection of peptides with semiconductor binding specificity for directed nanocrystal assembly," *Nature*, vol. 405, no. 6787, pp. 665–668, 2000.

[10] K. T. Nam, D.-W. Kim, P. J. Yoo, et al., "Virus-enabled synthesis and assembly of nanowires for lithium ion battery electrodes," *Science*, vol. 312, no. 5775, pp. 885–888, 2006.

[11] E. Dujardin, C. Peet, G. Stubbs, J. N. Culver, and S. Mann, "Organization of metallic nanoparticles using tobacco mosaic virus templates," *Nano Letters*, vol. 3, no. 3, pp. 413–417, 2003.

[12] M. Knez, M. Sumser, A. M. Bittner, et al., "Spatially selective nucleation of metal clusters on the tobacco mosaic virus," *Advanced Functional Materials*, vol. 14, no. 2, pp. 116–124, 2004.

[13] S.-Y. Lee, E. Royston, J. N. Culver, and M. T. Harris, "Improved metal cluster deposition on a genetically engineered tobacco mosaic virus template," *Nanotechnology*, vol. 16, no. 7, pp. S435–S441, 2005.

[14] S.-Y. Lee, J. Choi, E. Royston, D. B. Janes, J. N. Culver, and M. T. Harris, "Deposition of platinum clusters on surface-modified tobacco mosaic virus," *Journal of Nanoscience and Nanotechnology*, vol. 6, no. 4, pp. 974–981, 2006.

[15] T. Scheibel, R. Parthasarathy, G. Sawicki, X.-M. Lin, H. Jaeger, and S. L. Lindquist, "Conducting nanowires built by controlled self-assembly of amyloid fibers and selective metal deposition," *Proceedings of the National Academy of Sciences of the United States of America*, vol. 100, no. 8, pp. 4527–4532, 2003.

[16] F. Patolsky, Y. Weizmann, and I. Willner, "Actin-based metallic nanowires as bio-nanotransporters," *Nature Materials*, vol. 3, no. 10, pp. 692–695, 2004.

[17] R. Djalali, Y.-F. Chen, and H. Matsui, "Au nanowire fabrication from sequenced histidine-rich peptide," *Journal of the American Chemical Society*, vol. 124, no. 46, pp. 13660–13661, 2002.

[18] I. A. Banerjee, L. Yu, and H. Matsui, "Cu nanocrystal growth on peptide nanotubes by biomineralization: size control of Cu nanocrystals by tuning peptide conformation," *Proceedings of the National Academy of Sciences of the United States of America*, vol. 100, no. 25, pp. 14678–14682, 2003.

[19] I. A. Banerjee, L. Yu, and H. Matsui, "Room-temperature wurtzite ZnS nanocrystal growth on Zn finger-like peptide nanotubes by controlling their unfolding peptide structures," *Journal of the American Chemical Society*, vol. 127, no. 46, pp. 16002–16003, 2005.

[20] E. Royston, A. Ghosh, P. Kofinas, M. T. Harris, and J. N. Culver, "Self-assembly of virus-structured high surface area nanomaterials and their application as battery electrodes," *Langmuir*, vol. 24, no. 3, pp. 906–912, 2008.

[21] K. Srinivasan, S. Cular, V. R. Bhethanabotla, S. Y. Lee, and M. T. Harris, "Nanomaterial sensing layer based surface acoustic wave hydrogen sensors," in *Proceedings of IEEE Ultrasonics Symposium*, vol. 1, pp. 645–648, Rotterdam, The Netherlands, September 2005.

[22] R. J. Tseng, C. Tsai, L. Ma, J. Ouyang, C. S. Ozkan, and Y. Yang, "Digital memory device based on tobacco mosaic virus conjugated with nanoparticles.," *Nature Nanotechnology*, vol. 1, no. 1, pp. 72–77, 2006.

[23] H. Renner, G. Schlamp, I. Kleinwächter, et al., "Platinum group metals and compounds," in *Ullmann's Encyclopedia of Industrial Chemistry*, pp. 1–78, Wiley-VCH, 2001.

[24] K. Namba and G. Stubbs, "Structure of tobacco mosaic virus at 3.6 Å resolution: implications for assembly," *Science*, vol. 231, no. 4744, pp. 1401–1406, 1986.

[25] A. Klug, "The tobacco mosaic virus particle: structure and assembly," *Philosophical Transactions of the Royal Society B*, vol. 354, no. 1383, pp. 531–535, 1999.

[26] J.-S. Lim, S.-M. Kim, S.-Y. Lee, E. A. Stach, J. N. Culver, and M. T. Harris, "Quantitative study of Au(III) and Pd(II) ion biosorption on genetically engineered tobacco mosaic virus," *Journal of Colloid and Interface Science*, vol. 342, no. 2, pp. 455–461, 2010.

[27] R. Higuchi, B. Krummel, and R. K. Saiki, "A general method of in vitro preparation and specific mutagenesis of DNA fragments: study of protein and DNA interactions," *Nucleic Acids Research*, vol. 16, no. 15, pp. 7351–7367, 1988.

[28] T. H. Turpen, S. J. Reinl, Y. Charoenvit, S. L. Hoffman, V. Fallarme, and L. K. Grill, "Malarial epitopes expressed on the surface of recombinant tobacco mosaic virus," *Bio/Technology*, vol. 13, no. 1, pp. 53–57, 1995.

[29] J. A. Peck, C. D. Tait, B. I. Swanson, and G. E. Brown Jr., "Speciation of aqueous gold(III) chlorides from ultraviolet/visible absorption and Raman/resonance Raman spectroscopies," *Geochimica et Cosmochimica Acta*, vol. 55, no. 3, pp. 671–676, 1991.

[30] C. D. Tait, D. R. Janecky, and P. S. Z. Rogers, "Speciation of aqueous palladium(II) chloride solutions using optical spectroscopies," *Geochimica et Cosmochimica Acta*, vol. 55, no. 5, pp. 1253–1264, 1991.

[31] K. Fujiwara, A. Ramesh, T. Maki, H. Hasegawa, and K. Ueda, "Adsorption of platinum (IV), palladium (II) and gold (III) from aqueous solutions onto l-lysine modified crosslinked chitosan resin," *Journal of Hazardous Materials*, vol. 146, no. 1-2, pp. 39–50, 2007.

[32] B. Greene, M. Hosea, R. McPherson, M. Henzl, M. D. Alexander, and D. W. Darnall, "Interaction of gold(I) and gold(III) complexes with algal biomass," *Environmental Science and Technology*, vol. 20, no. 6, pp. 627–632, 1986.

[33] J.-H. Kim, W. W. Bryan, H.-W. Chung, C.-Y. Park, A. J. Jacobson, and T. R. Lee, "Gold, palladium, and gold-palladium alloy nanoshells on silica nanoparticle cores," *Applied Materials and Interfaces*, vol. 1, no. 5, pp. 1063–1069, 2009.

[34] J. W. Edington, *Practical Electron Microscopy in Materials Science*, N.V. Philips, Eindhoven, The Netherlands, 1991.

[35] *A Chart of Inner Shell Loss Edge Types and Energy*, Gatan Inc., 1985.